Single Cell Mechanotransduction and Its Modulation Analyzed by Atomic Force Microscope Indentation

Guillaume T. Charras and Mike A. Horton
The Bone and Mineral Center, The Rayne Institute, Department of Medicine, University College, London WC1E 6JJ, United Kingdom

ABSTRACT The skeleton adapts to its mechanical usage, although at the cellular level, the distribution and magnitude of strains generated and their detection are ill-understood. The magnitude and nature of the strains to which cells respond were investigated using an atomic force microscope (AFM) as a microindentor. A confocal microscope linked to the setup enabled analysis of cellular responses. Two different cell response pathways were identified: one, consequent upon contact, depended on activation of stretch-activated ion channels; the second, following stress relaxation, required an intact microtubular cytoskeleton. The cellular responses could be modulated by selectively disrupting cytoskeletal components thought to be involved in the transduction of mechanical stimuli. The F-actin cytoskeleton was not required for responses to mechanical strain, whereas the microtubular and vimentin networks were. Treatments that reduced membrane tension, or its transmission, selectively reduced contact reactions. Immunostaining of the cell cytoskeleton was used to interpret the results of the cytoskeletal disruption studies. We provide an estimate of the cellular strain magnitude needed to elicit intracellular calcium responses and propose a model that links single cell responses to whole bone adaptation. This technique may help to understand adaptation to mechanical usage in other organs.

INTRODUCTION

Bone is a structure finely tuned to its mechanical environment. This concept was introduced by Wolff in 1892 and reinforced by Koch's finding, in 1917, that trabecular orientations closely matched stress trajectories (cited from Martin and Burr, 1989). Peak strains measured in vivo on the bone surface by strain gauges (which measure average strain over a length of several millimeters) reach a maximum of 3000–4000 $\mu\epsilon$ during normal activity in many species (Lanyon and Smith, 1969). In a seminal experiment, Rubin and Lanyon (1984a) showed that bone mass could be maintained by applying a small number of physiological strain events, and increased when a higher number of loading cycles was applied. This suggested that bone adapts to its mechanical usage (Lanyon, 1992).

Strain detection in the skeleton is thought to be effected by bone-lining cells and osteocytes embedded within the bone matrix (Cowin et al., 1991; Lanyon, 1993). However, because bone is a composite material with multiple enclosed cavities (e.g., osteocyte lacunae, Haversian canals) and a complex architecture, the strain to which cells are subjected in vivo and to which they react remains unknown. Finite-element (FE) model reconstructions of microcomputed tomographies of bones offer a way of predicting strain within the bony tissue (van Rietbergen et al., 1999). Several studies have shown that strain applied to the bony tissue (millimeter scale) can result in severalfold larger strain levels around osteocyte lacunae (micrometer scale) (Hollister et al., 1994).

Cells can sense mechanical stimuli through mechanosensitive ion channels, integrin receptors, or tyrosine kinases (Sachs and Morris, 1998; Banes et al., 1995; Malek and Izumo, 1996). The exact mechanism involved and the downstream events may depend on the type of stimulation and is considered likely to also involve cell- or tissue-specific components. An early and quasi-ubiquitous response to mechanical stimuli is a rise in intracellular calcium concentration, and this signal can be transmitted to neighboring cells to sensitize a larger area of tissue. The cytoskeleton is a closely interwoven network of actin, tubulin, and intermediate filaments that modulates cell sensitivity to mechanical stimuli by adapting its structure to accommodate prolonged mechanical strains (Ko and McCulloch, 2000; Janmey, 1998). Cytoskeletal integrity is important for detection and transduction of mechanical strain and cellular elasticity (Ko and McCulloch, 2000; Wang, 1998; Rotsch and Radmacher, 2000). Among the many methods of applying a mechanical stimulus onto a single cell, only atomic force microscopy (AFM) enables a precise application of very low forces, the measurement of cell elasticity (Radmacher, 1997), minimal disruption to cells (Haydon et al., 1996), and the determination of cellular strain distributions during indentation (Charras et al., 2001).

In this study we sought to determine, at the single cell level, the characteristic strains to which osteoblastic cells respond to further understand the relationships between cell mechanics, the cytoskeleton, and mechanosensitivity. We quantified the mechanical strains needed to elicit intracellular calcium responses in primary osteoblasts. The proportion of reacting cells followed a dose-dependent curve with respect to applied strain. Intracellular calcium rises could be transmitted to neighboring cells. Calcium entry was investigated by using specific blockers of key elements of the calcium pathway, and cellular sensitivity was modulated by

Submitted December 18, 2001, and accepted for publication February 15, 2002.

Address reprint requests to Dr. Mike Horton, The Rayne Institute, 5 University Street, London WC1E 6JJ, UK. Tel.: 44-207-679-6169; Fax: 44-207-679-6219; E-mail: m.horton@ucl.ac.uk.

0006-3495/02/06/2970/12 $2.00

selectively disrupting cytoskeletal components previously shown to be involved in the transduction of mechanical stimuli. The effects of these drugs on cell morphology and organization were also investigated. These data led us to propose a model that integrates cellular exposure to mechanical strain, cytoskeletal integrity, and calcium-mediated cell signaling to link single-cell reactions to whole-bone adaptation. The use of AFM as an analytical tool of mechanical responses is likely to find applications in other cell/tissue systems that adapt to their mechanical environment in normal physiology or disease.

MATERIALS AND METHODS

Cell culture

Osteoblasts were isolated from the long bones of neonatal rats by mechanical disaggregation and cultured for 72 h at 37°C in an atmosphere of 5% CO_2 in air in DMEM (Gibco Life Technologies, Paisley, UK) supplemented with 10% FCS, 2% glutamine, 2% PS, 2% 1 M HEPES, pH 7.0.

Histological staining

Osteoblastic phenotype was ascertained by alkaline phosphatase staining as described in Herbertson and Aubin (1995) and the percentage of alkaline phosphatase positive cells was estimated by inspection of areas of red coloration.

Immunostaining and confocal microscopy

Immunostaining was performed as described in Nesbitt and Horton (1997). Briefly, the cells were fixed in a PBS solution containing 2% formaldehyde and 0.1% glutaraldehyde, and permeabilized in ice-cold Triton X-100 buffer for 5 min at 4°C. For the cytoskeletal triple stains, the cells were sequentially incubated with monoclonal anti-vimentin antibody (Sigma, St. Louis, MO) for 30 min, FITC-labeled goat anti-mouse Ig antibody (Dako, Glostrup, Denmark) for 30 min, Biotin-Phalloidin (Molecular Probes, Eugene, OR) for 45 min, Cy5-labeled Streptavidin (Amersham, Bucks, UK) for 45 min, rabbit polyclonal anti-α tubulin (Santa Cruz, Santa Cruz, CA) for 1 h, and TRITC-labeled swine anti-rabbit Ig antibody (Dako) for 30 min. For gap-junctional staining, the cells were incubated with monoclonal anti-connexin 43 (Cx-43) (Transduction Laboratories, Lexington, KY), a gap-junctional protein, for 30 min; FITC-labeled goat anti-mouse Ig antibody for 30 min; and rhodamine-phalloidin (Molecular Probes) for 30 min. All coverslips were imaged with a 100× oil-immersion objective on a Leica confocal microscope running TCS NT (Leica, Bensheim, Germany). Fluorescent images were sequentially collected in 0.4-μm steps with emission wavelengths of 488, 568, and 647 nm for FITC, TRITC, and Cy5 fluorophores, respectively. The images were then post-processed using Imaris software (Bitplane Ag, Zürich, Switzerland) on an SGI O_2 workstation (SGI, Mountain View, CA).

Functional gap junctional communication assay

This assay was performed as described by Yellowley et al. (2000). Briefly, cells were divided into two batches and cultured for 3 days. One batch was loaded with both 10 μM calcein-AM (Molecular Probes), a cytosolic marker, and 5 $\mu l \cdot ml^{-1}$ DiI (Vybrant red; Molecular Probes), a lipophilic membrane marker. The labeled cells were then detached by enzymatic digestion and a small drop of these was added to the unlabelled cell culture. Calcein was able to diffuse to other cells through gap junctions, whereas the membrane marker could not and was used to identify the parachuting cells.

Intracellular calcium measurements

Cells were incubated in medium for 1 h with 6 μM Fluo3-AM (Molecular Probes) and imaged in physiological buffer (127 mM NaCl, 5 mM KCl, 2 mM $MgCl_2$, 0.5 mM $Na_2H\ PO_4$, 2 mM $CaCl_2$, 5 mM $NaHCO_3$, 10 mM glucose, 10 mM HEPES, 0.1% BSA, pH 7.4). For experiments with Gd^{3+}, the same buffer but without phosphate or carbonate was used (Sachs and Morris, 1998). Intracellular calcium levels were assessed via a confocal scanning laser microscope (Bio-Rad Radiance 2000, Biorad, Hemel Hempstead, UK) fitted onto a Nikon TE300 (Nikon, Kanagawa, Japan) inverted microscope. A 20× Nikon Neoplan objective was used for imaging. The Bio-Rad time course software was used to capture images of the cells at intervals of 1 s for as long as desired. Pinhole diameter was chosen such that the thickness of the optical slice did not exceed cell height. The temporal evolution of the fluorescence intensity could be assessed at several locations within and between cells.

Atomic force microscopy

A Thermomicroscopes Explorer (Thermomicroscopes, Sunnyvale, CA) interfaced onto our inverted microscope was used to mechanically stimulate the cells (Lehenkari et al., 2000). Soft cantilevers ($k = 0.032\ N \cdot m^{-1}$, no. 1520, Thermomicroscopes) were calibrated in air before experimentation (Hutter and Bechhoefer, 1994). Glass beads (diameters between 10 and 30 μm, Sigma) were glued onto the cantilevers (Lehenkari et al., 2000) to act as indentors, and their diameter was measured before experimentation.

Experimental procedure

A well-loaded cell was chosen and the AFM positioned above it. The confocal microscope data collection was started and, after 30 s, the cantilever was approached toward the cell surface. After 20 s in contact with the cell, a force-distance curve was taken to enable determination of cell elasticity at the location of indentation. The AFM cantilever was then retracted from the surface and the data collection was continued for a further 40 s to monitor any stress relaxation reactions. In some experiments, a second stimulus with a larger force was applied 30 s later.

Spontaneous calcium waves

To assess the frequency of spontaneous increases in intracellular calcium, optical fields covered with cells were monitored for 200 s each. All cells and reacting cells were counted for each experiment. This yielded a probability of reacting spontaneously per unit time.

Measurement of material properties

Cell elasticities were evaluated as described in Radmacher (1997) and modified by Charras et al. (2001). The cellular Poisson ratio was assumed to be 0.3 (Maniotis et al., 1997) and a theoretical model was fitted to the experimental force-distance curve yielding cell elasticity using a custom-written program running under Pv-Wave (Visual Numerics, Boulder, CO) on an SGI O_2 workstation.

Determining cellular strains

Knowing the cell elasticity and the force applied, the strains applied on the surface of the cell by a rigid spherical indentor can be computed. The radial surface strains $\bar{\epsilon}_{rr}$ (Johnson, 1985; Charras et al., 2001) are:

$$\overline{\varepsilon_{rr}}(r) = \frac{\partial \overline{u_r}(r)}{\partial r} = \frac{(1-2\nu)(1+\nu)}{3E}\frac{a^2}{r^2}p_0\left\{1-\left(1-\frac{r^2}{a^2}\right)^{3/2}\right\} - \frac{(1-2\nu)(1+\nu)}{E}p_0\left(1-\frac{r^2}{a^2}\right)^{1/2}, \quad r \le a \qquad (1)$$

$$\overline{\varepsilon_{rr}}(r) = \frac{\partial \overline{u_r}(r)}{\partial r} = \frac{(1-2\nu)(1+\nu)}{3E}\frac{a^2}{r^2}p_0, \quad r > a \qquad (2)$$

$$a = \left(\frac{3}{4}\frac{PR(1-\nu^2)}{E}\right)^{1/3} \qquad (3)$$

$$p_0 = \frac{3}{2}\frac{P}{\pi a^2} \qquad (4)$$

Where u_r is the radial displacement, ν the Poisson ratio, E the Young's modulus, a the radius of contact between the indentor and the cell, p_0 the pressure at the center of indentation, R the indentor radius, and P the total force applied.

The radial surface strain distribution has both a tensile (positive) and a compressive (negative) component and was calculated for each cell using a custom-written program. FE modeling showed that maximal radial strains were located on the cell surface and that maximal tangential strains were of similar magnitude to peak radial strains, whereas peak vertical strains were approximately threefold higher (Charras et al., 2001). Because the cellular material was assumed to be linear, maximal tangential and vertical strains evolved in proportion to maximal radial strains, and these can be used as an indicator of cell strain state.

Inhibitor studies

For each inhibitor the experiments were conducted in the same way as the controls. A very large force (>10 nN) was applied to obtain a large number of expected reactions. Single inhibitor concentrations were selected based upon accepted maximally effective values from the literature. In all cases there was no evidence of cellular toxicity. For cytoskeletal modification using drugs, post hoc immunostaining established the selectivity of action (Fig. 4 and data not shown).

Calcium entry pathway

To investigate calcium entry, the cells were incubated with inhibitors of the key elements of the entry pathways. Extracellular calcium entry was investigated by adding 5 mM EGTA (Calbiochem, CA) to the imaging medium and adjusting the pH to 7.4. To ascertain that cells in calcium-free medium were not depleted in calcium, 5 μM bradykinin (Novabiochem, Switzerland) was used as a positive control stimulus. Mechanosensitive cation channels were blocked with 50 μM Gd^{3+} (Sigma) (Sachs and Morris, 1998). Intracellular calcium stores were depleted by incubating the cells with 1 μM thapsigargin (Sigma). The phosphatidyl-inositol-specific phospholipase C (PI-PLC) pathway was blocked with 20 μM Et-18-OCH_3 (Sigma). Voltage-activated calcium channels were blocked by incubating the cells with 10 μM verapamil (Sigma). The involvement of tyrosine kinases was assessed by incubating the cells with 50 μM genistein (Calbiochem). All compounds were added to the culture medium 30 min before stimulation and were present in the imaging medium throughout the experiment.

Cytoskeletal modulation of mechanical signal transduction

To elucidate the importance of the cytoskeleton in the transduction of mechanical stimuli, compounds were used to selectively modify the cytoskeletal components. Cytochalasin B (5 μM, Sigma) was used to disrupt F-actin. Jasplakinolide (0.1 μM, Molecular Probes) was used to aggregate F-actin filaments. Nocodazole (10 μM, Molecular Probes) was used to depolymerize microtubules. Paclitaxel (0.1 μM, Calbiochem) was used to inhibit microtubular depolymerization. Acrylamide (4 mM, BDH Chemicals, UK) was used to dissolve vimentin (Wang, 1998). Diamide (0.5 mM, Sigma) was used to disrupt the links between spectrin filaments and the F-actin network (Adachi and Iwasa, 1997). Membrane tension was decreased by incubating with 5 $\mu l \cdot ml^{-1}$ DiI, an amphiphilic compound that incorporates into the cell membrane (Raucher and Sheetz, 2000). All reagents were added to the medium 30 min before the experiment, except acrylamide (1 h before) and DiI (15 min before), and were present throughout the experiment.

Morphological effects of cytoskeletal disruption

To examine the effect of cytoskeletal disruption on cellular organization and better understand the changes in intracellular calcium reactions, the cells were examined with triple immunostaining of F-actin, microtubules, and vimentin. The effects on cell height and volume were examined by loading live cells with 2.5 μM calcein-AM or 10 μM CFMDA (Molecular Probes) and taking a z-stack of images of the cells before and after cytoskeletal disruption using a Bio-Rad confocal microscope with a 100× oil-immersion objective. The cell heights and volumes before and after treatment were derived from the confocal images using a custom-written program based on the techniques described in Guilak (1994).

Data analysis and statistics

Each experimental recording of calcium intensity was checked for intracellular calcium increases. When these occurred, their timing was compared to the noted times of contact and lift-off of the cantilever. If the reaction coincided with the time of indentation and the intracellular calcium rise was greater than the baseline by five standard deviations of the noise, the experiment was deemed positive. The reacting cells were classified into three groups: those that reacted only when contact with the cantilever was first established (touchdown group, or TD); those that reacted only when the cantilever was lifted off the cell surface (lift-off group, or LO), and those that reacted in both cases (TDLO group). For every stimulated cell, data analysis yielded cell elasticity, radial surface strains, and the presence or not of a reaction.

The strain dependence of intracellular reactions was examined in two ways, both for the tensile and for the compressive components of the strain distribution. First, the data were grouped into a total of four strain-ranges and the percentage of cells reacting on TD, LO, or TDLO was computed for each range. The differences between ranges were assessed with a one-way ANOVA on the nonreacting cells. Results were deemed significant if $p < 0.05$. Second, the data were binned into 5 millistrain strain-ranges and the percentage of cells reacting was computed for each strain range. A sigmoid curve weighted according to the number of cells in each range was fitted to the percentage cells reacting. The r^2 value gave an indication of the goodness of fit. At zero strain, the percentage of spontaneously reacting cells was used. To provide estimates of the proportion of

cells reacting at very high strain, data from an experiment on primary osteoblasts stimulated by micropipette poking (Xia and Ferrier, 1992) was incorporated into the graph. The strain elicited by micropipette poking was estimated by assuming $R = 2$ μm and an indentation depth of 0.5 μm.

To assess whether the calcium transient amplitude was correlated with applied strain, we normalized the data with the baseline intensity and plotted the percent increase in calcium as a function of applied strain. A line was fitted to the data and the r^2 value gave an indication of the goodness of fit.

To examine inhibitor effects, the applied strains were computed for each cell examined and using the dose response curve as a probability curve, a probability for reaction on LO, TD, or TDLO was computed. This yielded an expected number of reactions on TD and LO, which was compared to the number of reactions experimentally observed using a Chi-square test. The results were deemed statistically significant if $p < 0.01$.

Differences in elasticity, applied strain, or indentation depth between cell populations were examined using Student's *t*-test. Cell heights or volumes after cytoskeletal disruption were compared to untreated controls using Student's *t*-test. Changes in height and volume for the untreated population were compared to zero using Student's *t*-test. Results were deemed statistically significant when $p < 0.05$.

RESULTS

Phenotype

After 72 h in culture, ~80% of the bone-derived cells were alkaline phosphatase positive (data not shown) and used as a source of "osteoblasts."

Spontaneous calcium reactions

A total of 20 optical fields with a total of 2624 cells were examined for 200 s each; 36 cells (1.3%) reacted, yielding a probability of spontaneously reacting during a given 1-s interval of $p = 6 \times 10^{-5}$.

Mechanically stimulated calcium reactions

Cells were mechanically stimulated by AFM and reacted either on contact (TD) or lift-off (LO) (Fig. 1, *A–D* show a typical experiment, and Fig. 1 *E* shows the time course of calcium intensity in the stimulated cell). Only a small amount of cellular material was displaced by indentation (Fig. 1 *F*).

A total of 231 experiments were performed on 122 cells. Increases in intracellular calcium were noted in 111 cases (48.0%). The increase in intracellular calcium was noted only on contact (TD) in 29 cases (12.6%), only on lift-off (LO) in 51 cases (22.0%), and both on contact and lift-off (TDLO) in 31 cases (13.4%). The elasticity of the reacting and nonreacting cells were not significantly different ($E = 3175 \pm 3260$ Pa, $p = 0.63$), whereas the forces applied were ($p < 0.001$). No sign of adhesion between indentor and cell was noted in the AFM retraction curves. The average depth of indentation in nonreacting cells (0.65 μm) was significantly lower than for stress relaxation reactions (0.86 μm, $p = 0.02$) and contact reactions (1.11 μm, $p < 0.001$). The average maximal strain applied to nonreacting cells in tension (23,565 $\mu\epsilon$) and compression (−35,436 $\mu\epsilon$) was significantly lower than that applied to cells reacting through stress relaxation (27,633/−41,554 $\mu\epsilon$, $p = 0.004$), which was in turn significantly lower than that applied to cells reacting on contact (32,488/−48,846 $\mu\epsilon$, $p = 0.03$). The estimated applied strains during micropipette poking were 96,000/−95,000 $\mu\epsilon$ and 96% of cells reacted (Xia and Ferrier, 1992).

The weighted sigmoid (Fig. 1 *G*) fit the data well ($r^2 = 0.87$) and reached half-maximum at 25,000 $\mu\epsilon$. When examined with a one-way ANOVA (Fig. 1 *H*), the number of nonreacting cells in the range [0; +20] was significantly different from the [+20; +30] range ($p = 0.01$). The [+30; +40] and the [+40; +65] ranges were also significantly different ($p = 0.04$). However, the difference between the [+20; +30] and [+30; +40] ranges failed to reach significance ($p = 0.07$). The amplitude of the calcium transients did not correlate with applied strain for either contact reactions ($r^2 = 0.04$) or stress relaxation reactions ($r^2 = 0.005$) (data not shown).

Propagation of signal and presence of functional gap-junctions and gap-junctional proteins

Propagation of the intracellular calcium rise was observed in 4.7% of cases. Fig. 2, *A–D* show the propagation of the signal from a stimulated cell to neighboring cells. The cells possessed functional gap-junctions (Fig. 2, *F* and *G*) and gap-junctional protein Cx-43 was situated at the junctions between cells (Fig. 2 *E*).

Pathway inhibitors (Fig. 3 *A*)

EGTA significantly inhibited cellular reactions ($p < 0.001$, $n = 26$). Bradykinin was used as a positive control stimulus and all cells reacted when it was added to calcium-free medium ($n = 21$). Gd^{3+} completely inhibited contact reactions (−100%) and had a minor effect on stress relaxation reactions (−40%) ($p < 0.001$, $n = 25$). Thapsigargin completely inhibited reactions on lift-off (−100%) but only had a minor effect on contact reactions (−36%) ($p = 0.003$, $n = 20$). Et-18-OCH_3 significantly inhibited cellular reactions ($p < 0.001$, $n = 22$). Verapamil inhibited cellular reactions significantly ($p = 0.004$, $n = 23$). Genistein had no significant effect on cellular reactions ($p = 0.15$, $n = 26$). None of these treatments modified cell elasticity ($p > 0.2$).

Cytoskeletal disrupting drugs (Fig. 3 *B*)

Paclitaxel significantly inhibited cellular reactions ($p = 0.002$, $n = 47$), showing a more marked decrease in contact reactions (−63%) than in lift-off reactions (−31%). No-

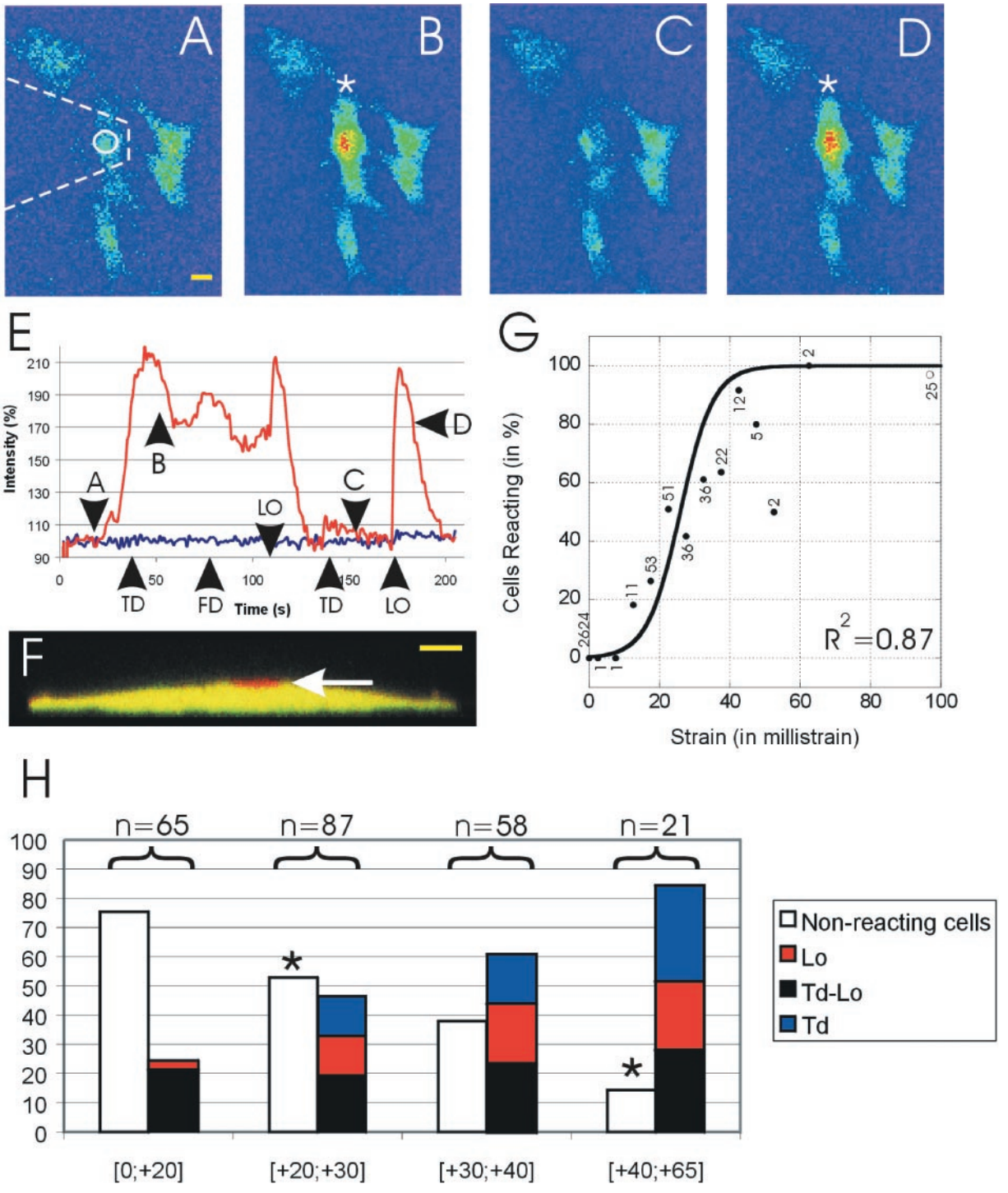

FIGURE 1 (*A–D*) Osteoblasts respond to a mechanical stimulus by a rise in intracellular calcium. (*A*) The cell has not yet been contacted. (*B*) The cell has reacted after contact (TD). It further reacts twice, after the force-distance (FD) curve and after the cantilever is lifted off the cell (LO). The cell is then allowed to rest for 30 s before being indented with a larger force (*C*). (*D*) The cantilever has been lifted off the cell and there has been another increase in intracellular calcium. Bar = 20 μm. (*E*) Calcium intensity time course of the experiment and the times of contact, lift-off, and force-distance curves are indicated. (*F*) A zx-scan of a cell loaded with calcein-AM. One image was taken before indentation (*red*) and one during indentation (*green*), and both images were superimposed. The area displaced by indentation can be seen in red. Bar = 10 μm. (*G*) A curve fitted to the cellular reactions as a function of the strain applied. The goodness of fit was $r^2 = 0.87$. The numbers refer to the number of cells in each strain group. The open circle refers to data from Xia and Ferrier (1992). (*H*) The cellular reactions as a function of strain and reactions to TD, LO, or both. The nonreacting cells were compared for each category with a one-way ANOVA. Asterisks indicate columns significantly different from the column to its left. The number of cells in each group is indicated above the columns.

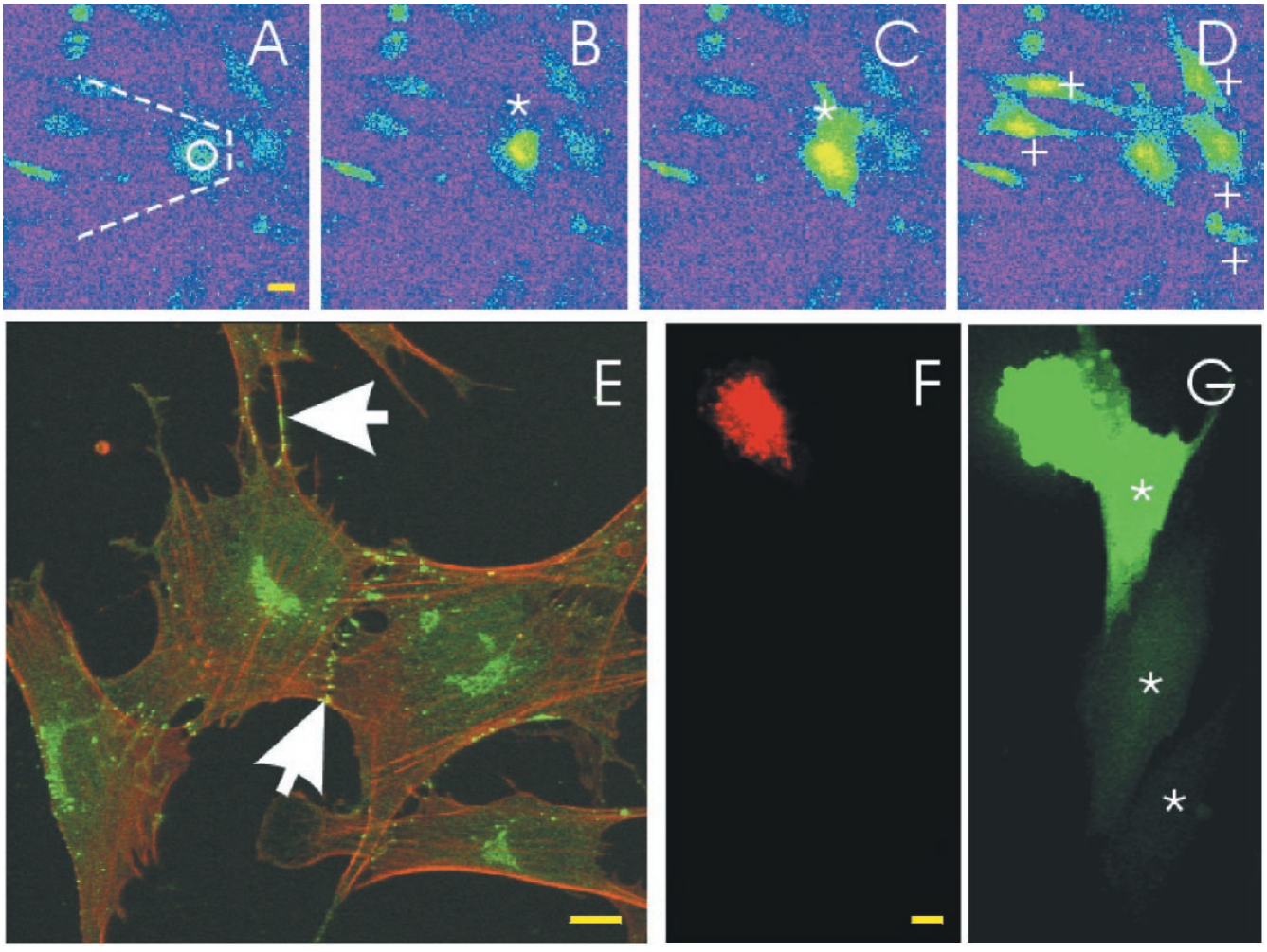

FIGURE 2 (*A–D*) Transmission of strain-induced calcium increases to adjacent cells. (*A*) The cell has been contacted. (*B*) The cell (indicated by an asterisk) has reacted to mechanical stimulation after lifting the cantilever. The area that was beneath the cantilever shows an increased calcium concentration ($t = 0$ s). (*C*) The calcium signal has spread to the whole cell ($t = 1$ s). (*D*) The signal has been passed on to five neighboring cells (indicated by crosses) ($t = 10$ s). Bar = 20 μm. (*E*) The localization of Cx-43 (*green*) within osteoblastic cells and at cell-cell contact points (*arrows*) after a 72-h culture period. F-Actin is shown in red. Bar = 10 μm. (*F* and *G*) Osteoblasts cultured for 72 h can form functional gap-junctions. The cell in (*F*) was loaded with DiI (*red*) that does not diffuse to other cells, and with calcein-AM (*green*) that does. In (*G*), the calcein has diffused to three other cells (indicated by asterisks). Bar = 10 μm.

codazole significantly inhibited cellular reactions ($p < 0.001$, $n = 22$). Neither paclitaxel nor nocodazole had a significant effect on cell elasticity ($p = 0.92$ and 0.36, respectively). Both cytochalasin B and jasplakinolide halved cell elasticity ($p = 0.001$ and $p = 0.04$) but had no significant effect on cellular reactions ($p = 0.04$ in both cases, $n = 43$ and $n = 29$, respectively). Acrylamide showed a trend toward reducing cell elasticity ($p = 0.07$) and reduced contact reactions (−92%), but not stress relaxation reactions (+20%) ($p = 0.001$, $n = 28$). Diamide had no effect on cell elasticity ($p = 0.32$), but significantly altered cellular reactions ($p = 0.002$, $n = 28$, touchdown −74% and lift-off −30%). DiI had no effect on cell elasticity ($p = 0.5$), but had a biphasic effect on cellular reactions, decreasing contact reactions (−54%) and increasing stress relaxation reactions (+50%) ($p = 0.008$, $n = 30$).

Confocal microscopy of the cytoskeleton after disruption

In untreated cells (Fig. 4 *A*), vimentin and tubulin formed a fibrous network that extended throughout the cell, showing a degree of colocalization that was particularly marked around the nucleus (data not shown). Tubulin, but not vimentin, was present at cellular extremities. Actin showed a distinct organization: stress fibers spanned the cell running parallel to one another. After a 72 h culture the cell profile was flattened and elongated, reaching maximal height around the nucleus (data not shown).

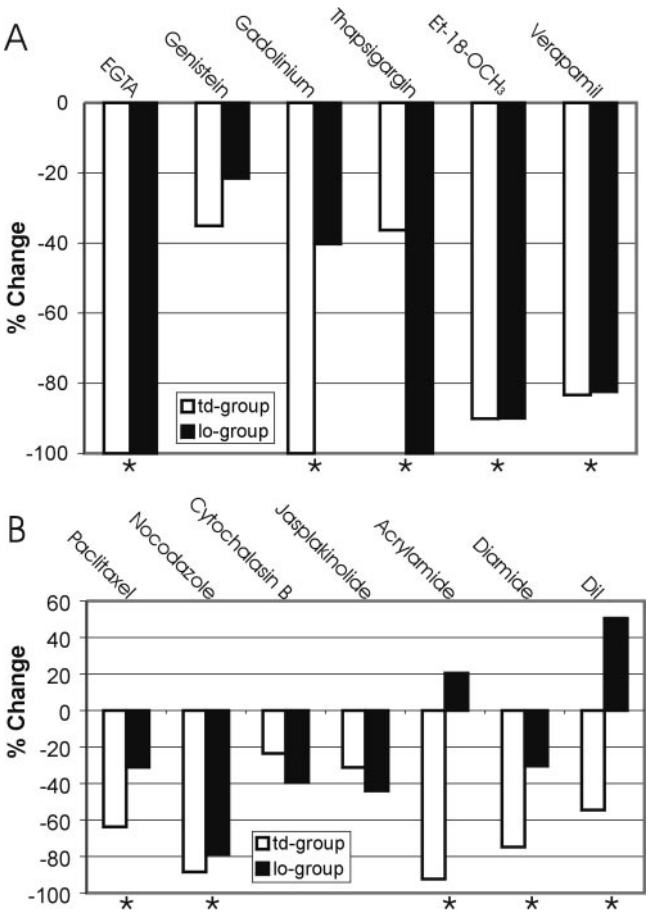

FIGURE 3 Effect of inhibitors on the proportion of cells reacting to mechanical strain by a calcium increment. (*A*) Effect of pathway inhibitors on the proportion of cells reacting. (*B*) Effect of modifying the cytoskeletal integrity on the proportion of cells reacting. The open bars show touchdown responses and the filled bars reactions upon lift-off. Asterisks indicate significant differences to control experiments.

Incubation with acrylamide (Fig. 4 *B*) disrupted the vimentin network and large areas of the cell became devoid of vimentin and microtubules, but the actin network seemed unaffected. Acrylamide reduced maximum cell height but had no effect on cell volume (Table 1).

Treatment with cytochalasin B (Fig. 4 *C*) disrupted the F-actin network and led to the rearrangement of the microtubular and vimentinous networks, which remained closely associated. After treatment, the cells assumed a rounded profile (Fig. 4 *E*). Jasplakinolide aggregated F-actin into actinous "blobs," severely disrupted the vimentin and microtubular networks, and caused rounding up of the cells (data not shown and Table 1).

Nocodazole (Fig. 4 *D*) dissolved the microtubules and had no notable effect on the F-actin network. The vimentinous network was greatly disrupted and reorganized perpendicular to actin stress fibers. Nocodazole-treated cells assumed a flattened morphology (Fig. 4 *F* and Table 1). Paclitaxel increased the density of microtubules but had no noticeable effect on the vimentin or actin networks (data not shown). Paclitaxel-treated cells were higher, but showed the same profile as control cells (Fig. 4 *G* and Table 1). Diamide had no noticeable effect on cytoskeletal organization (data not shown), but caused cellular rounding (Fig. 4 *H* and Table 1).

DISCUSSION

In this study we have examined the ability of osteoblasts to respond to directly applied mechanical stimuli using an AFM indentor. We estimate the cellular strain magnitude required to elicit an intracellular calcium response and show that the proportion of cells reacting increases with increasing strain. Cells reacted either directly after contact or once the load was removed. The calcium response was transmissible to neighboring cells, and these possessed connexins and functional gap-junctions. Calcium entry after contact and lift-off occurred via different pathways and resulted from the detection of different components of strain. The F-actin cytoskeleton was not required for cellular responses to strain, whereas the microtubular and the vimentin networks were.

The proportion of cells responding to mechanical stimulation was dependent on the magnitude of applied strain; 50% of the cells responded for maximal tensile strains of 25,000 $\mu\epsilon$ and compressive strains of $-40{,}000$ $\mu\epsilon$. The magnitude of strain to which bone-lining cells and osteocytes are subjected in vivo remains controversial. In vivo peak strains, averaged over several millimeters by strain gauge measurement, on the surface of long bones range from 2100 to 3000 $\mu\epsilon$ in most mammals (Rubin and Lanyon, 1984b; Burr et al., 1996). Because bone is a composite material with many embedded cavities (e.g., Haversian canals, osteocyte lacunae, Volkmann's canals) and a complex micro-architecture, strain magnitude within bone would not be expected to be the same as on the bone surface (Cowin et al., 1991). In an FE model of a canine proximal femur during the stance phase of walking strain distributions were nonuniform, with cortical strains of 958 $\mu\epsilon$ and maximal trabecular strains of 3731 $\mu\epsilon$ (van Rietbergen et al., 1999). Since bone was modeled as a linear material, strenuous exercise (3000 $\mu\epsilon$ on the cortex surface) would generate maximal strains of 9346 $\mu\epsilon$ in trabeculae. When the composite nature of bone was taken into account, strains around osteocyte lacunae were $\sim$10-fold larger than those applied on tissue level (Hollister et al., 1994). In line with these observations, populations of osteoblasts derived from the periosteum reacted to lower strains than those derived from the bone interior (3000 $\mu\epsilon$ vs. 10,000 $\mu\epsilon$) when subjected to substrate stretch (Jones et al., 1991). A study of the strain history at mid-diaphysis has shown that high strain events ($>$1000 $\mu\epsilon$) occur only a few times a day (Fritton et al., 2000). From our AFM data, together with the

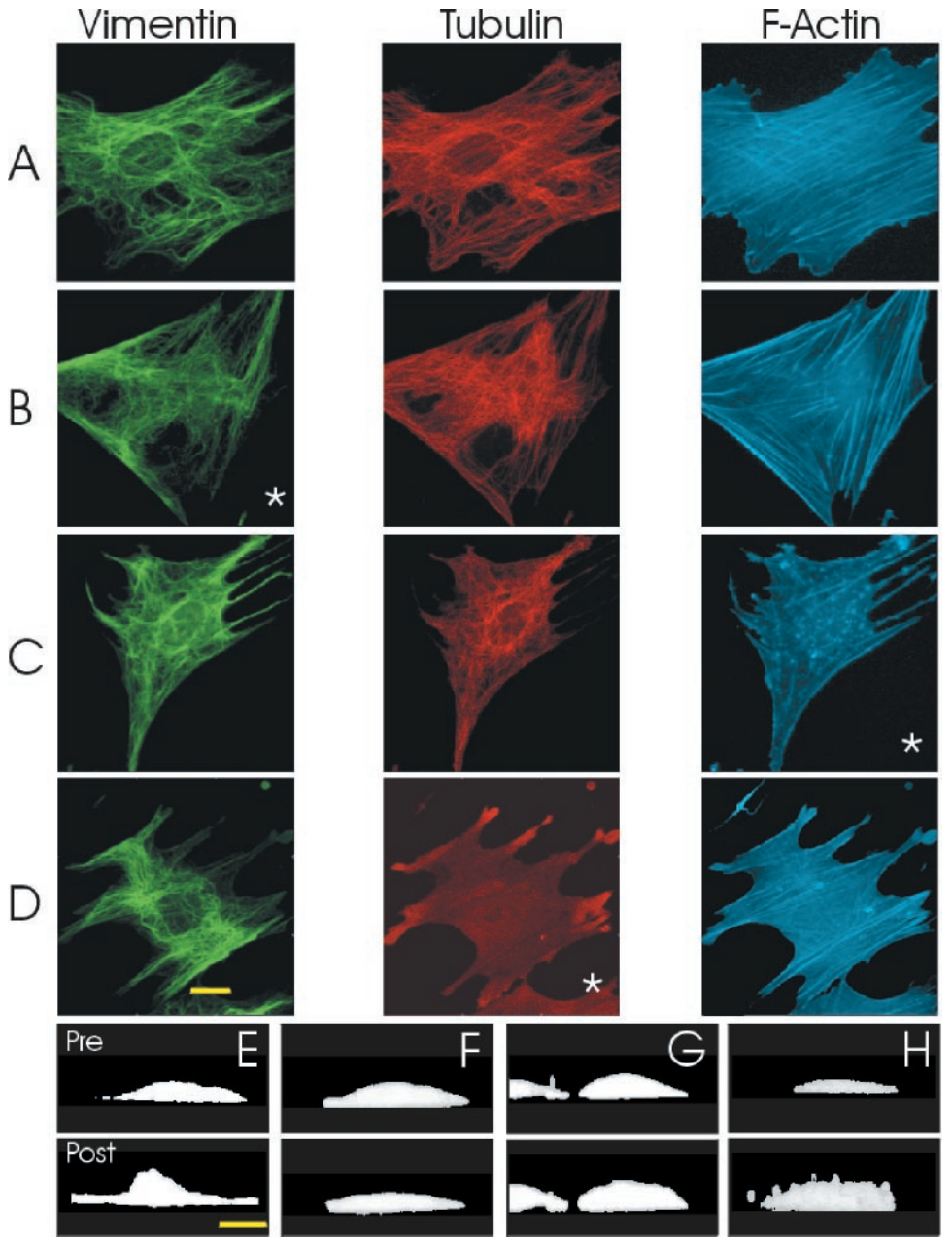

FIGURE 4 Effect of cytoskeletal treatments on cytoskeletal organization and cellular profile. (*A–D*) Vimentin (*green*), tubulin (*red*), and F-actin (*blue*) are shown as through focus confocal images for each reagent. Asterisks indicate where a treatment is "expected" to produce a cytoskeletal modification. Bar = 10 μm. (*A*) Acrylamide; (*B*) cytochalasin B; (*C*) jasplakinolide; (*D*) nocodazole; (*E*) paclitaxel. (*E–H*) zx-Confocal sections of calcein-AM loaded live osteoblasts before and after treatment. Bar = 10 μm. (*E*) Cytochalasin B; (*F*) nocodazole; (*G*) paclitaxel; (*H*) diamide.

strain amplification due to the bone matrix, few events a day would reach a magnitude sufficient to induce cell reactions.

Different genes are transcribed in response to different frequencies of calcium transients (Dolmetsch et al., 1998; Li et al., 1998). Thus in lymphoid cells, infrequent oscillations favored the expression of genes transcribed by nuclear factors with long persistence times in the nucleus, and frequent oscillations additionally transcribed genes whose factors had shorter persistence times. In bone, four daily strain events are necessary to maintain bone mass, whereas a higher number of strain events leads to bone formation (Rubin and Lanyon, 1984a). Signal transmission to surrounding cells ensures a concerted reaction to high local strain. If the signal is infrequent (e.g., four times daily), transcription of regulatory genes would ensue (e.g., inhibitors of osteoclast formation, such as osteoprotegerin); if the signal is more frequent, transcription of the genes necessary for osteoblast activation and matrix deposition could be undertaken. Thus, mechanical strain, signal

TABLE 1 Effect of cytoskeletal disruption on cell height and cell volume

	n	Average Change in Maximum Height (μm)	*p*	Average Change in Volume (μm^3)	*p*
Untreated	25	−0.29	0.39*	−205	0.27
Cytochalasin B	15	3.93	<0.01	2003	<0.01
Jasplakinolide	17	0.86	0.02	348	0.02
Nocodazole	19	−1.07	0.09	−253	0.46
Paclitaxel	25	1.05	<0.01	533	<0.01
Acrylamide	19	0.97	<0.01	114	0.17
Diamide	32	0.99	0.01	451	0.02

n, Number of cells examined for each treatment; *p*, result of Student's *t*-test comparing the changes in height or volume to the untreated controls.
*The untreated controls were compared to a zero change using Student's *t*-test.

transduction, and the regulation of bone formation versus removal could be integrated.

How do the strains needed to elicit intracellular calcium responses by AFM indentation compare to those induced by substrate stretch or fluid shear? The interpretation of data from substrate stretching experiments must be circumspect because some stretching systems elicit fluid movement that may impose significant strains on cells in addition to substrate stretch (Brown et al., 1998; You et al., 2000). Although the qualitative observations from such studies remain well founded, the actual level of strain elicited may not be reliably known. Moreover, they are bulk measurements that do not take into account the averaging of heterogeneous responses. Upregulation of a variety of cellular constituents at strains lower than those shown to elicit an intracellular calcium rise in our study have been reported (Zaman et al., 1997; Fermor et al., 1998; Kaspar et al., 2000; Jones et al., 1991), and others needed comparable strain levels (Meazzini et al., 1998; Toma et al., 1997; Wozniak et al., 2000; Jones et al., 1991). Fluid shear has also been used to stimulate osteoblastic cells (Hung et al., 1996; Ajubi et al., 1999), but these studies are difficult to compare to ours because cellular strains are unknown. Our study differed from the above on a number of grounds. First, we applied strain directly to the cell surface and no probe-cell adhesion was detected. This is different from substrate stretch, where the cell is stimulated through focal adhesion complexes that act as point-adhesions of the cell membrane to the substrate. This may have major consequences for signal transduction and detection threshold. Second, we only applied one or two strain episodes, in contrast with several hundred during substrate stretch or oscillating fluid flow experiments. In our study, a small proportion of intracellular calcium rises was transmitted to neighboring cells; furthermore, our cells possessed functional gap-junctions (Fig. 2) and the time lags between reactions of neighboring cells (10–30 s) were consistent with signal propagation through gap junctions (Jorgensen et al., 1997). When osteoblasts were stimulated by poking with micropipettes (applying an uncontrolled and substantially larger strain: 96,000 $\mu\epsilon$ vs. 25,000 $\mu\epsilon$ for AFM), calcium transients were readily propagated (Xia and Ferrier, 1992; Jorgensen et al., 1997). In contrast, cells stimulated by pulling magnetically on adherent microbeads (with only a 4.4 pN force), did not propagate calcium transients (Wu et al., 1999). Therefore, higher strain magnitudes may activate cellular signaling and further amplify the tissue response via gap-junctional propagation.

Distinct calcium entry pathways were involved in the transduction of contact and stress relaxation reactions, and these responded to different components of the applied strain (Fig. 5). Calcium transient magnitude did not correlate with applied strain magnitude, suggesting internal signal amplification. In our experiments, intracellular calcium responses involved both extracellular and intracellular calcium, as observed in other experiments involving mechanical perturbation such as fluid shear (Ajubi et al. (1999); Hung et al. (1996)) and micropipette poking (Xia and Ferrier (1992); Hung et al. (1996)). PI-PLCs were also involved as in fluid shear (Ajubi et al. (1999); Hung et al. (1996)) and substrate stretch experiments (Jones et al. (1991)). However, contrary to results reported by Hung et al. (1996), voltage-activated calcium channels were also involved. Contact reaction and stress relaxation transduction pathways were shown to differ through the selective block of contact reactions by Gd^{3+} and of stress relaxation reactions by thapsigargin. This suggests that the high membrane tensile strains, present on the cell surface during indentation (Charras et al., 2001), open stretch-activated cation channels. This would lead to a local depolarization of the cell membrane and open voltage-activated calcium channels. Calcium entry may then be potentiated by a calcium-induced calcium release and the activation of calcium-sensitive PLCs (Berridge et al., 2000), as indicated in Fig. 5 *A*. This mechanism is similar to that proposed to mediate responses to micropipette aspiration (Kirber et al., 2000). The presence of a large compressive vertical strain component under the area of indentation (Charras et al., 2001), and the inhibition of stress relaxation reactions by nocodazole (Fig. 3 *B*), suggests that microtubule-bound kinases or GTPases may be activated during the dynamic relaxation of the cytoskeleton after indentation (Malek and Izumo, 1996; Janmey, 1998). This may in turn activate the inositol-1,4,5-

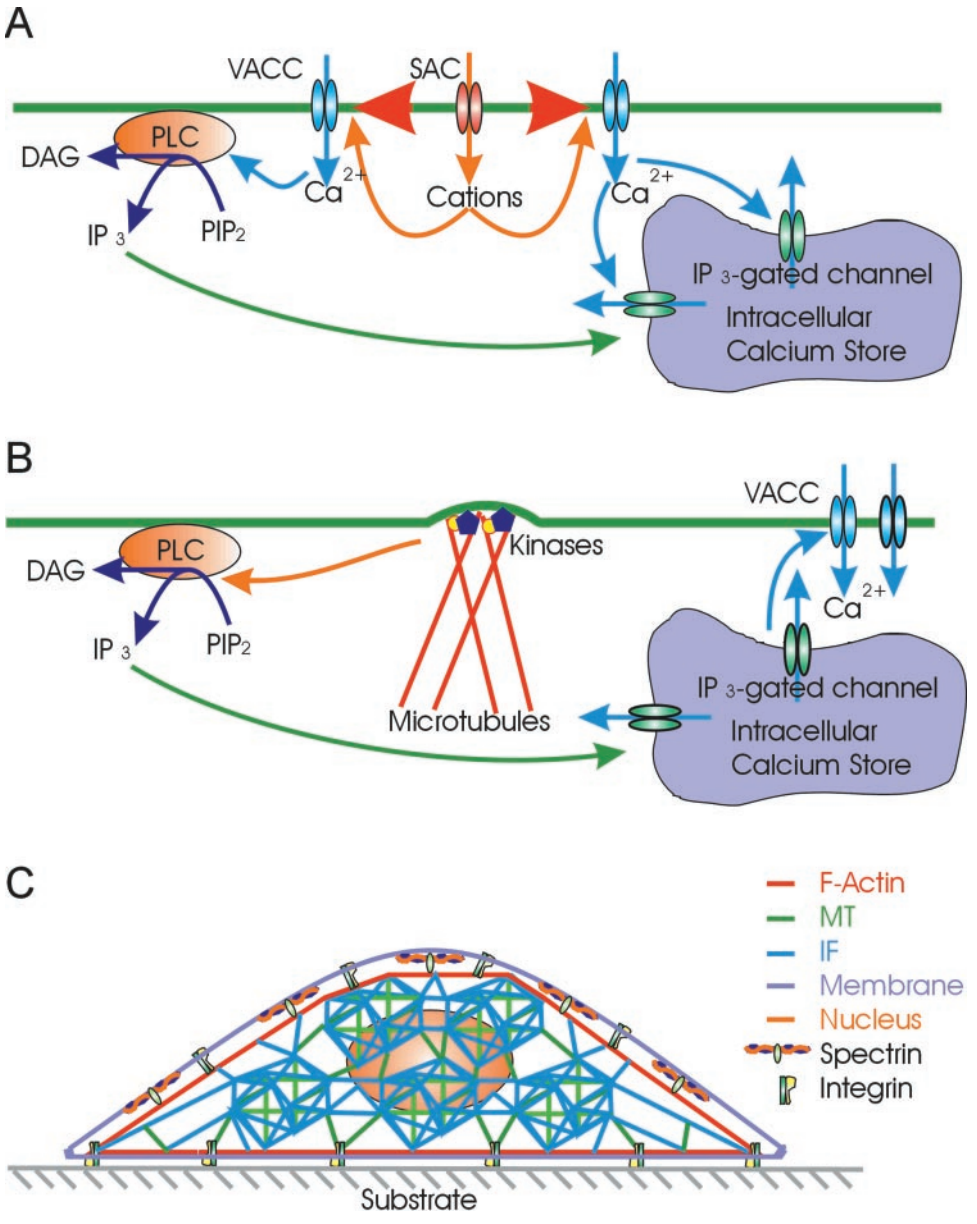

FIGURE 5 Calcium entry pathways for contact and stress relaxation reactions. Mechanical model of the cell. (*A*) Tension applied to the cell membrane (*red arrowheads*) at indentor contact (touchdown) opens stretch-activated cation channels (SAC). Inflowing cations cause local depolarization of the cell membrane, which triggers the opening of voltage-sensitive Ca^{2+} channels (VACC). Ca^{2+} can then activate either calcium-sensitive PLCs or IP_3 receptor channels leading to the release of calcium from intracellular calcium stores. (*B*) As the load is removed from the cell membrane (lift-off) the microtubules relax, and while regaining their original conformation bring microtubule-bound proteins (e.g., kinases) into contact and activate them. These may then trigger an IP_3-dependent pathway that could be potentiated by voltage-sensitive Ca^{2+} channels. (*C*) Mechanical model of a cell. The integrins and spectrin filaments tether the cell membrane to the F-actin network. The F-actin network anchors the whole cell to the substrate via focal adhesion complexes and applies pre-stress onto the cell interior. In the cell interior, the microtubules (MT) and the intermediate filaments (IF) are arranged in a tensegrity structure where the MTs act as load-bearing trusses and IFs as tensile stiffeners. The cell nucleus is linked to the internal tensegrity structure. PIP_2: phosphatidyl inositol-4,5-bisphosphate; DAG: diacyl glycerol.

triphosphate (IP_3) pathway and voltage-activated channels (Fig. 5 *B*).

Our cytoskeletal disruption data lead us to propose a model of the cell for resisting and detecting mechanical forces (Fig. 5 *C*). Therein, vimentin and tubulin would form the tensegrity structure of the cell, in which the nucleus is embedded, with the microtubules being the load-bearing elements and intermediate-filaments the tensile stiffeners (Ingber, 1993). F-actin stress fibers would serve as guy wires, anchoring the internal tensegrity unit to the substrate and applying pre-stress to it. The membrane would also apply pre-stress to the cell interior through to its intrinsic

tension, and spectrin filaments would tether the membrane to the F-actin network and participate in the generation of membrane tension (Sokabe et al., 1991). Indeed, F-actin did not seem critical in mechanotransduction (Fig. 3 *B*; also seen in other cell types: Niggel et al. (2000); Wu et al. (1999)). In contrast, F-actin played a crucial role in modulating cellular elasticity (in agreement with Rotsch and Radmacher (2000) and Wang (1998)) and maintaining cell shape (Fig. 4 *E*, Table 1). These results suggest that F-actin filaments apply a pre-stress onto the cell interior, possibly through the action of myosin motors. The microtubular network played an essential role in the transduction of mechanical stimuli (in agreement with fluid shear experiments on endothelial cells by Malek and Izumo (1996)). It was intimately connected to vimentin, but not to the F-actin network (Fig. 4 *D*). Upon disruption of the microtubular network, vimentin filaments disappeared from the cell periphery and regrouped in the cell center, organizing themselves perpendicularly to the actin filaments (Fig. 4 *D*). Disruption of the vimentin network increased cell height (though less than when F-actin was disrupted, Table 1) suggesting that, although vimentin applies some pre-stress, most of the pre-stress is applied by F-actin. Furthermore, vimentin played a crucial role in the transduction of contact reactions (Fig. 3 *B*). Neither disruption of tubulin or vimentin, nor stabilization of tubulin, had any significant effect on cellular elasticity when probed with AFM (in agreement with Rotsch and Radmacher (2000)). However, when elasticity was probed via magnetic microbeads bound to the cytoskeleton via integrin transmembrane receptors, tubulin- and vimentin-filaments played a major role in the capacity of the cytoskeleton to resist mechanical forces (Wang, 1998). Disruption of the spectrin/fodrin filaments increased cell height (Fig. 4 *H*, Table 1), but had no effect on actin, tubulin, or vimentin distribution within the cells (data not shown). Spectrin disruption selectively inhibited contact reactions (Fig. 3 *B*) thereby underlining its role in the generation of membrane pre-tension and in modulating stretch-activated channel sensitivity. Reducing membrane tension, by increasing its area through incorporation of the amphiphilic compound DiI (Raucher and Sheetz, 2000), resulted in a change in cell sensitivity to mechanical strain (Fig. 3 *B*). Indeed, a decrease in membrane tension would reduce the pre-tension exerted on the stretch-activated channels, and hence reduce their sensitivity. A lower tension in the cell membrane would also offer less resistance to the relaxation of the internal tensegrity structure as it regains its shape after deformation.

In summary, we have demonstrated that osteoblastic cells respond to mechanical strain and for the first time, estimate the threshold cellular strain needed to elicit an intracellular calcium reactions. Two different pathways for detection of mechanical stimuli co-existed. One pathway, upon indentation, relied on stretch-activated cation channels for the first step of the transduction cascade and was sensitive to tensile radial strains in the cell membrane. In contrast, the other, upon removal of stimulus, depended on microtubule-bound proteins and was sensitive to the vertical strain component. We propose a mechanically coherent model for detection of whole bone strain at the cellular level and its transduction to generate whole bone level changes. Furthermore, we believe that our AFM-based technique may be fruitfully applied to other cells and tissues that are subjected to mechanical strain, and adapt to it, such as the blood vessel wall, cardiac and skeletal muscle, or the auditory system. Indeed, knowledge of the detection thresholds of different cell types will be pivotal in understanding the physiological regulation of downstream events in response to mechanical stimulation.

This work was supported by a Johnson and Johnson COSAT grant and by a program grant from the Wellcome Trust to MAH.

REFERENCES

Adachi, M. and K. H. Iwasa. 1997. Effect of diamide on force generation and axial stiffness of the cochlear outer hair cell. *Biophys. J.* 73: 2809–2818.

Ajubi, N. E., J. Klein-Nulend, M. J. Alblas, E. H. Burger, and P. J. Nijweide. 1999. Signal transduction pathways involved in fluid flow-induced PGE2 production by cultured osteocytes. *Am J. Physiol. Endocrinol. Metab.* 276:E171–E178.

Banes, A. J., M. Tsuzaki, J. Yamamoto, T. Fischer, B. Brigman, T. Brown, and L. Miller. 1995. Mechanoreception at the cellular level: the detection, interpretation, and diversity of responses to mechanical signals. *Biochem. Cell Biol.* 73:349–365.

Berridge, M. J., P. Lipp, and M. D. Bootman. 2000. The versatility and universality of calcium signalling. *Nat. Rev. Mol. Cell Biol.* 1:11–21.

Brown, T. D., M. Bottlang, D. R. Pedersen, and A. J. Banes. 1998. Loading paradigms—intentional and unintentional—for cell culture mechanostimulus. *Am. J. Med. Sci.* 316:162–168.

Burr, D. B., C. Milgrom, D. Fyhrie, M. Forwood, M. Nyska, A. Finestone, S. Hoshaw, E. Saiag, and A. Simkin. 1996. In vivo measurement of human tibial strains during vigorous activity. *Bone.* 18:405–410.

Charras, G. T., P. P. Lehenkari, and M. A. Horton. 2001. Atomic force microscopy can be used to mechanically stimulate osteoblasts and evaluate cellular strain distributions. *Ultramicroscopy.* 86:85–95.

Cowin, S. C., L. Moss-Salentijn, and M. L. Moss. 1991. Candidates for the mechanosensory system in bone. *J. Biomech. Eng.* 113:191–197.

Dolmetsch, R. E., K. Xu, and R. S. Lewis. 1998. Calcium oscillations increase the efficiency and specificity of gene expression. *Nature.* 392: 933–936.

Fermor, B., R. Gundle, M. Evans, M. Emerton, A. Pocock, and D. Murray. 1998. Primary human osteoblast proliferation and prostaglandin E2 release in response to mechanical strain in vitro. *Bone.* 22:637–643.

Fritton, S. P., K. J. McLeod, and C. T. Rubin. 2000. Quantifying the strain history of bone: spatial uniformity and self-similarity of low-magnitude strains. *J. Biomech.* 33:317–325.

Guilak, F. 1994. Volume and surface area measurement of viable chondrocytes in situ using geometric modeling of serial confocal sections. *J. Microsc.* 173:245–256.

Haydon, P. G., R. Lartius, V. Parpura, and S. P. Marchese-Ragona. 1996. Membrane deformation of living glial cells using atomic force microscopy. *J. Microsc.* 182:114–120.

Herbertson, A., and J. E. Aubin. 1995. Dexamethasone alters the subpopulation make-up of rat bone marrow stromal cell cultures. *J. Bone Miner. Res.* 10:285–294.

Hollister, S. J., J. M. Brennan, and N. Kikuchi. 1994. A homogenization sampling procedure for calculating trabecular bone effective stiffness and tissue level stress. *J. Biomech.* 27:433–444.

Hung, C. T., F. D. Allen, S. R. Pollack, and C. T. Brighton. 1996. Intracellular Ca^{2+} stores and extracellular Ca^{2+} are required in the real-time Ca^{2+} response of bone cells experiencing fluid flow. *J. Biomech.* 29:1411–1417.

Hutter, J. L., and J. Bechhoefer. 1994. Calibration of atomic-force microscope tips. *Rev. Sci. Instrum.* 64:1868–1873.

Ingber, D. E. 1993. Cellular tensegrity: defining new rules of biological design that govern the cytoskeleton. *J. Cell Sci.* 104:613–627.

Janmey, P. A. 1998. The cytoskeleton and cell signaling: component localization and mechanical coupling. *Physiol Rev.* 78:763–781.

Johnson, K. L. 1985. Contact Mechanics. Cambridge University Press, Cambridge, New York, Melbourne.

Jones, D. B., H. Nolte, J. G. Scholubbers, E. Turner, and D. Veltel. 1991. Biochemical signal transduction of mechanical strain in osteoblast-like cells. *Biomaterials.* 12:101–110.

Jorgensen, N. R., S. T. Geist, R. Civitelli, and T. H. Steinberg. 1997. ATP- and gap junction-dependent intercellular calcium signaling in osteoblastic cells. *J. Cell Biol.* 139:497–506.

Kaspar, D., W. Seidl, C. Neidlinger-Wilke, A. Ignatius, and L. Claes. 2000. Dynamic cell stretching increases human osteoblast proliferation and CICP synthesis but decreases osteocalcin synthesis and alkaline phosphatase activity. *J. Biomech.* 33:45–51.

Kirber, M. T., A. Guerrero-Hernandez, D. S. Bowman, K. E. Fogarty, R. A. Tuft, J. J. Singer, and F. S. Fay. 2000. Multiple pathways responsible for the stretch-induced increase in Ca^{2+} concentration in toad stomach smooth muscle cells. *J. Physiol.* 524:3–17.

Ko, K. S., and C. A. McCulloch. 2000. Partners in protection: interdependence of cytoskeleton and plasma membrane in adaptations to applied forces. *J. Membr. Biol.* 174:85–95.

Lanyon, L. E. 1992. Control of bone architecture by functional load bearing. *J. Bone Miner. Res.* 7(Suppl. 2):S369–S375.

Lanyon, L. E. 1993. Osteocytes, strain detection, bone modeling and remodeling. *Calcif. Tissue Int.* 53(Suppl. 1):S102–S106.

Lanyon, L. E., and R. N. Smith. 1969. Measurements of bone strain in the walking animal. *Res. Vet. Sci.* 10:93–94.

Lehenkari, P. P., G. T. Charras, A. Nykänen, and M. A. Horton. 2000. Adapting atomic force microscopy for cell biology. *Ultramicroscopy.* 82:289–295.

Li, W., J. Llopis, M. Whitney, G. Zlokarnik, and R. Y. Tsien. 1998. Cell-permeant caged InsP3 ester shows that Ca^{2+} spike frequency can optimize gene expression. *Nature.* 392:936–941.

Malek, A. M., and S. Izumo. 1996. Mechanism of endothelial cell shape change and cytoskeletal remodeling in response to fluid shear stress. *J. Cell Sci.* 109:713–726.

Maniotis, A. J., C. S. Chen, and D. E. Ingber. 1997. Demonstration of mechanical connections between integrins, cytoskeletal filaments, and nucleoplasm that stabilize nuclear structure. *Proc. Natl. Acad. Sci. U.S.A.* 94:849–854.

Martin, R. B., and D. B. Burr. 1989. Structure, Function, and Adaptation of Compact Bone. Raven Press, New York.

Meazzini, M. C., C. D. Toma, J. L. Schaffer, M. L. Gray, and L. C. Gerstenfeld. 1998. Osteoblast cytoskeletal modulation in response to mechanical strain in vitro. *J. Orthop. Res.* 16:170–180.

Nesbitt, S. A., and M. A. Horton. 1997. Trafficking of matrix collagens through bone-resorbing osteoclasts. *Science.* 276:266–269.

Niggel, J., W. Sigurdson, and F. Sachs. 2000. Mechanically induced calcium movements in astrocytes, bovine aortic endothelial cells and C6 glioma cells. *J Membr. Biol.* 174:121–134.

Radmacher, M. 1997. Measuring the elastic properties of biological samples with the AFM. *IEEE Eng. Med. Biol. Mag.* 16:47–57.

Raucher, D., and M. P. Sheetz. 2000. Cell spreading and lamellipodial extension rate is regulated by membrane tension. *J. Cell Biol.* 148: 127–136.

Rotsch, C., and M. Radmacher. 2000. Drug-induced changes of cytoskeletal structure and mechanics in fibroblasts: an atomic force microscopy study. *Biophys. J.* 78:520–535.

Rubin, C. T., and L. E. Lanyon. 1984b. Dynamic strain similarity in vertebrates; an alternative to allometric limb bone scaling. *J. Theor. Biol.* 107:321–327.

Rubin, C. T., and L. E. Lanyon. 1984a. Regulation of bone formation by applied dynamic loads. *J. Bone Joint Surg. [Am.]* 66:397–402.

Sachs, F., and C. E. Morris. 1998. Mechanosensitive ion channels in nonspecialized cells. *Rev. Physiol Biochem. Pharmacol.* 132:1–77.

Sokabe, M., F. Sachs, and Z. Q. Jing. 1991. Quantitative video microscopy of patch clamped membranes stress, strain, capacitance, and stretch channel activation. *Biophys. J.* 59:722–728.

Toma, C. D., S. Ashkar, M. L. Gray, J. L. Schaffer, and L. C. Gerstenfeld. 1997. Signal transduction of mechanical stimuli is dependent on microfilament integrity: identification of osteopontin as a mechanically induced gene in osteoblasts. *J. Bone Miner. Res.* 12:1626–1636.

van Rietbergen, B., R. Muller, D. Ulrich, P. Ruegsegger, and R. Huiskes. 1999. Tissue stresses and strain in trabeculae of a canine proximal femur can be quantified from computer reconstructions. *J. Biomech.* 32: 443–451.

Wang, N. 1998. Mechanical interactions among cytoskeletal filaments. *Hypertension.* 32:162–165.

Wozniak, M., A. Fausto, C. P. Carron, D. M. Meyer, and K. A. Hruska. 2000. Mechanically strained cells of the osteoblast lineage organize their extracellular matrix through unique sites of alphavbeta3-integrin expression. *J. Bone Miner. Res.* 15:1731–1745.

Wu, Z., K. Wong, M. Glogauer, R. P. Ellen, and C. A. McCulloch. 1999. Regulation of stretch-activated intracellular calcium transients by actin filaments. *Biochem. Biophys. Res. Commun.* 261:419–425.

Xia, S. L., and J. Ferrier. 1992. Propagation of a calcium pulse between osteoblastic cells. *Biochem. Biophys. Res. Commun.* 186:1212–1219.

Yellowley, C. E., Z. Li, Z. Zhou, C. R. Jacobs, and H. J. Donahue. 2000. Functional gap junctions between osteocytic and osteoblastic cells. *J. Bone Miner. Res.* 15:209–217.

You, J., C. E. Yellowley, H. J. Donahue, Y. Zhang, Q. Chen, and C. R. Jacobs. 2000. Substrate deformation levels associated with routine physical activity are less stimulatory to bone cells relative to loading-induced oscillatory fluid flow. *J. Biomech. Eng.* 122:387–393.

Zaman, G., R. F. Suswillo, M. Z. Cheng, I. A. Tavares, and L. E. Lanyon. 1997. Early responses to dynamic strain change and prostaglandins in bone-derived cells in culture. *J. Bone Miner. Res.* 12:769–777.